

Supporting Information

Molecular dynamics simulations reveal the mechanism of graphene oxide nanosheet towards the inhibition of A β ₁₋₄₂ peptide aggregation

Yibo Jin, Yunxiang Sun, Yujie Chen, Jiangtao Lei, Guanghong Wei*

Department of Physics, State Key Laboratory of Surface Physics, Key Laboratory for Computational Physical Sciences (Ministry of Education), 220 Handan Road, Shanghai 200433, People's Republic of China

*Corresponding author: Guanghong Wei, E-mail: ghwei@fudan.edu.cn

This material contains two supplemental tables and twelve supplementary figures.

Two supplemental tables:

Table S1: Temperature (K) list used in the 54-replica REMD simulations of A β ₄₂-dimer system:

306.30	308.16	310.03	311.91	313.80	315.70	317.60	319.51	321.44
323.37	325.32	327.26	329.22	331.19	333.16	335.14	337.13	339.14
341.15	343.17	345.20	347.24	349.29	351.35	353.41	355.49	357.58
359.67	361.78	363.90	366.08	368.22	370.37	372.52	374.69	376.86
379.05	381.24	383.45	385.66	387.89	390.12	392.37	394.62	396.89
399.17	401.45	403.75	406.06	408.38	410.71	413.05	415.41	417.77

Table S2: Temperature (K) list used in the 54-replica REMD simulations of A β ₄₂-dimer+GO system:

308.24	310.09	311.96	313.83	315.71	317.60	319.50	321.40	323.32
325.24	327.18	329.12	331.07	333.04	335.01	336.99	338.98	340.98
342.98	345.00	347.02	349.06	351.11	353.16	355.23	357.30	359.39
361.48	363.58	365.70	367.82	369.96	372.10	374.25	376.42	378.59
380.78	382.98	385.18	387.40	389.63	391.87	394.11	396.37	398.65
400.93	403.22	405.52	407.83	410.16	412.49	414.84	417.19	419.56

Twelve supplementary figures:

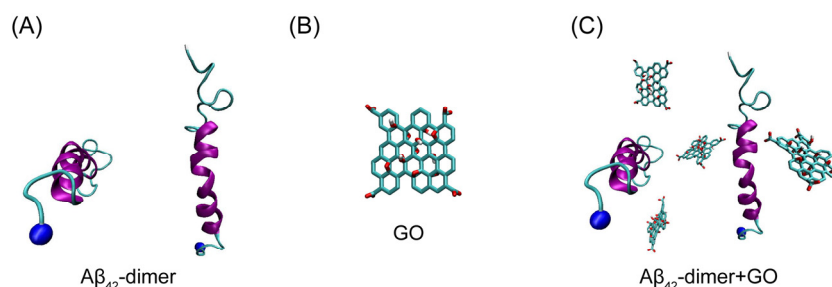


Fig. S1 The initial structure of the $A\beta_{1-42}$ ($A\beta_{42}$ for short) dimer ($A\beta_{42}$ -dimer system), the chemical structure of a GO nanosheet and the initial state of the $A\beta_{42}$ dimer with four pieces of GO nanosheets ($A\beta_{42}$ -dimer+GO system). (A) The $A\beta_{42}$ monomer taken from the NMR derived structure (PDB ID: 1Z0Q). (B) The chemical structure of a GO nanosheet. The GO nanosheet is in a stick representation. (C) The initial state of the $A\beta_{42}$ dimer with four pieces of GO nanosheets. The $C\alpha$ positions of D1 residues are represented by a ball.

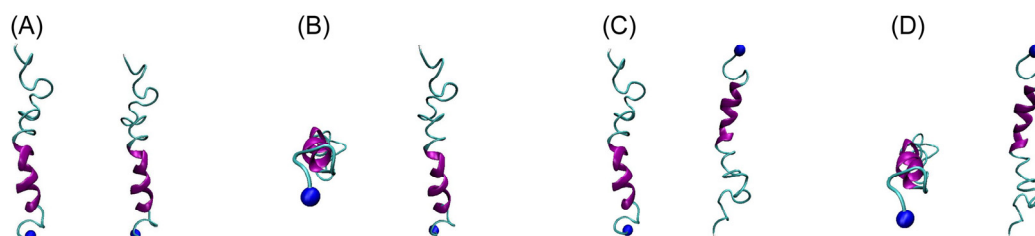


Fig. S2 The initial conformation of $A\beta_{42}$ dimer used for our REMD simulations: (A) dimer with parallel orientation, (B) (D) dimer with cross orientation, (C) dimer with anti-parallel orientation.

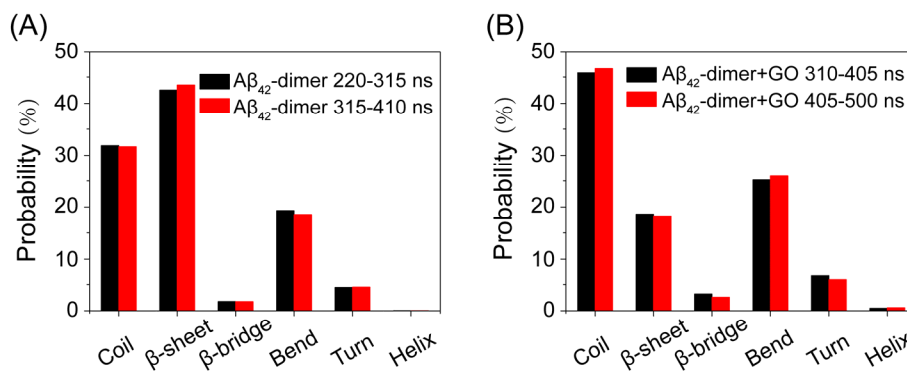


Fig. S3 The averaged secondary structure probability for the $A\beta_{42}$ dimer system (A) using 220-315 ns and 315-410 ns intervals and $A\beta_{42}$ dimer with GO nanosheets system (B) using 310-405 ns and 405-500 ns intervals, respectively.

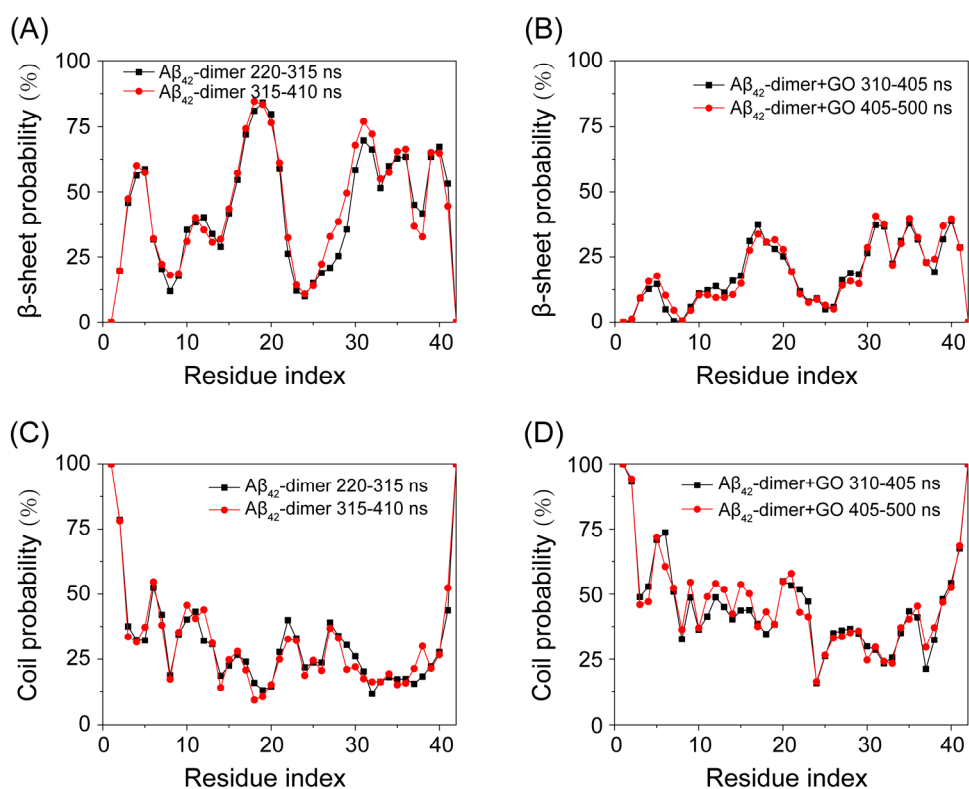


Fig. S4 Residue-based β -sheet and coil probability in REMD runs with the time intervals of 220-315 ns and 315-410 ns for $A\beta_{42}$ -dimer system (A, C) and 310-405 ns and 405-500 ns for $A\beta_{42}$ -dimer+GO system (B, D).

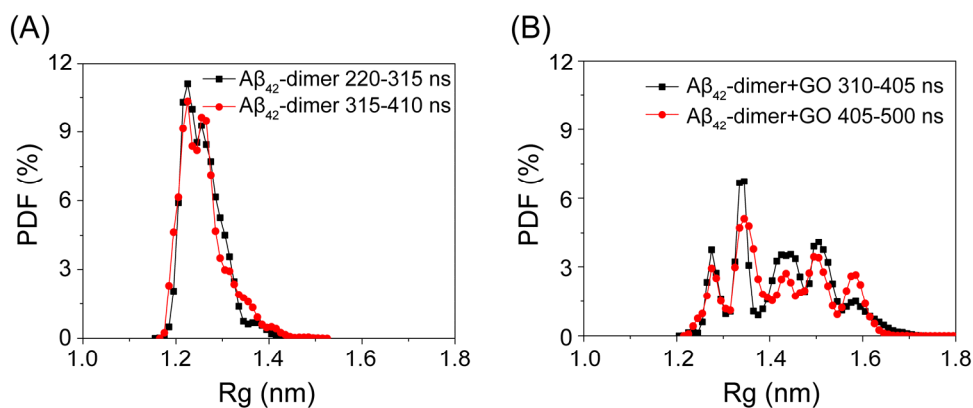


Fig. S5 The probability density function (PDF) of radius of gyration (R_g) for the $A\beta_{42}$ -dimer system (A) using 220-315 ns and 315-410 ns intervals and $A\beta_{42}$ -dimer+GO system (B) using 310-405 ns and 405-500 ns intervals, respectively.

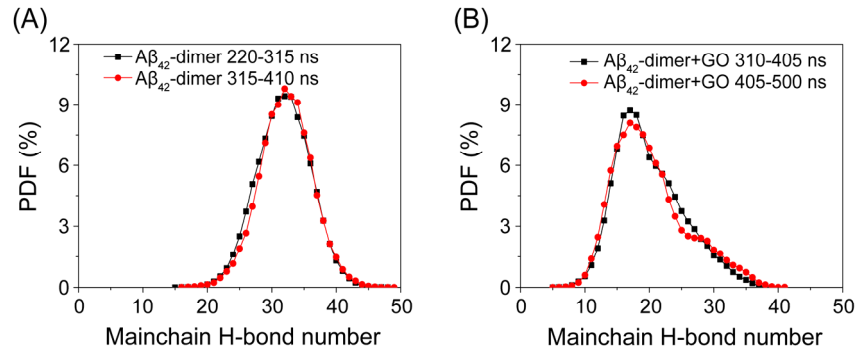


Fig. S6 The number of mainchain hydrogen bonds (H-bond) for the Aβ₄₂-dimer system (A) using 220-315 ns and 315-410 ns intervals and Aβ-dimer+GO system (B) using 310-405 ns and 405-500 ns intervals, respectively.

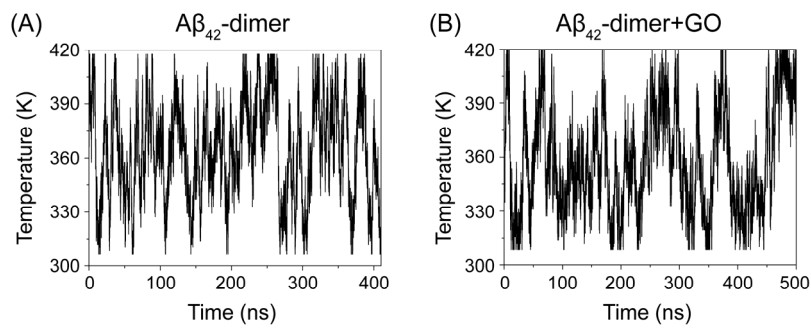


Fig. S7 The time evolution of temperature swapping of one representative replica in temperature space for Aβ₄₂-dimer system (A) and Aβ₄₂-dimer+GO system (B).

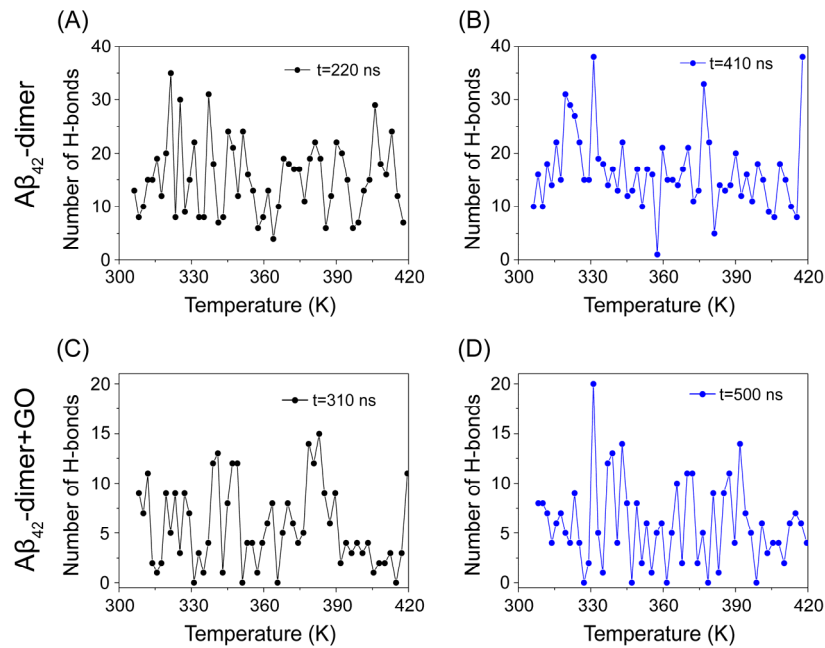


Fig. S8 Number of inter-chain H-bonds of the 54 replicas from 306 to 417 K at t=220 and 340 ns for Aβ₄₂-dimer (A, B) and from 308 to 419 K at t=310 and 500 ns Aβ₄₂-dimer+GO (C, D) systems.

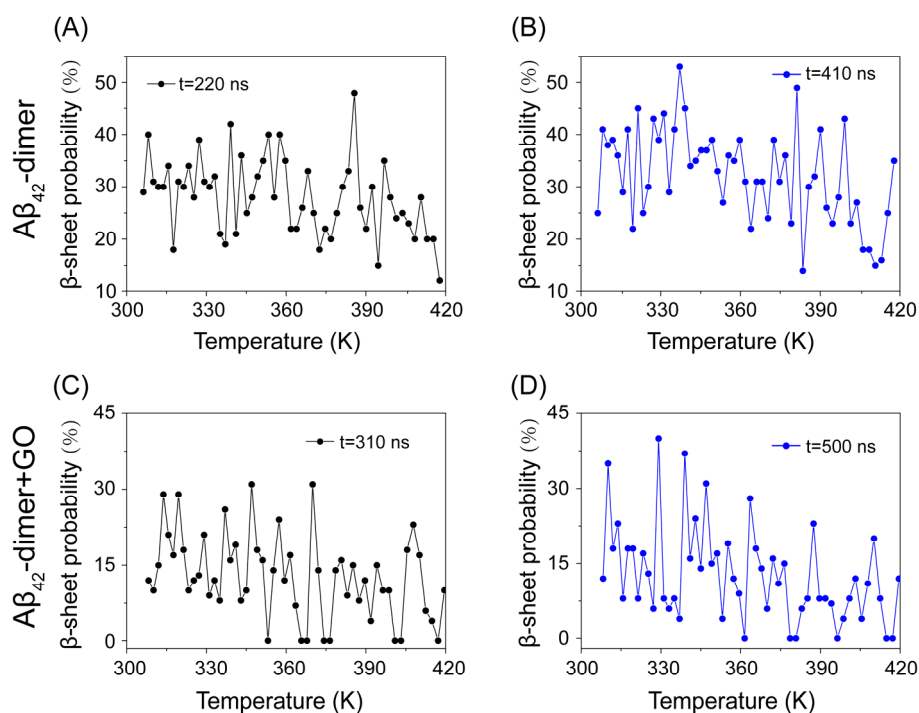


Fig. S9 β -sheet probability of the 54 replicas from 306 to 417 K at $t=220$ and 410 ns for $\text{A}\beta_{42}$ -dimer (A, B) and from 308 to 419 K at $t=310$ and 500 ns $\text{A}\beta_{42}$ -dimer+GO (C, D) systems.

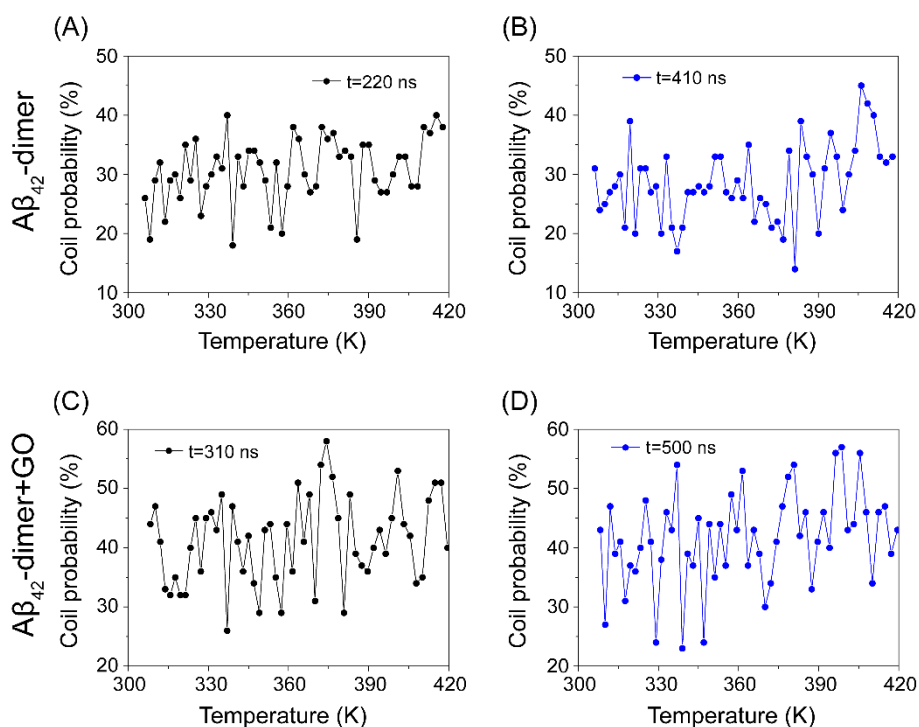


Fig. S10 Coil probability of the 54 replicas from 306 to 417 K at $t=220$ and 410 ns for $\text{A}\beta_{42}$ -dimer (A, B) and from 308 to 419 K at $t=310$ and 500 ns $\text{A}\beta_{42}$ -dimer+GO (C, D) systems.

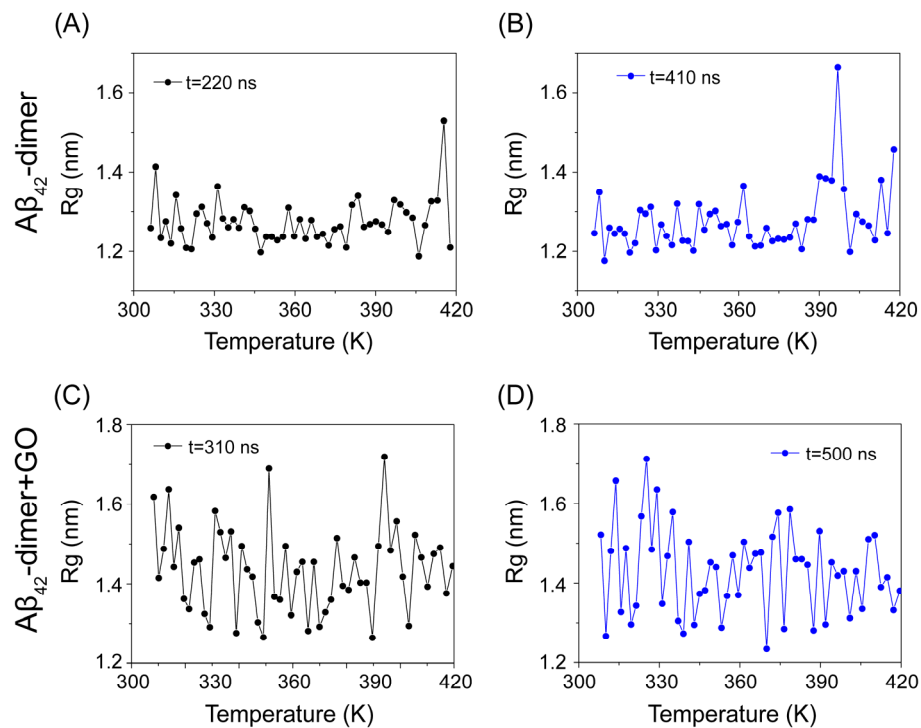


Fig. S11 R_g of the 54 replicas from 306 to 417 K at $t=220$ and 410 ns for $A\beta_{42}$ -dimer (A, B) and from 308 to 419 K at $t=310$ and 500 ns for $A\beta_{42}$ -dimer+GO (C, D) systems.

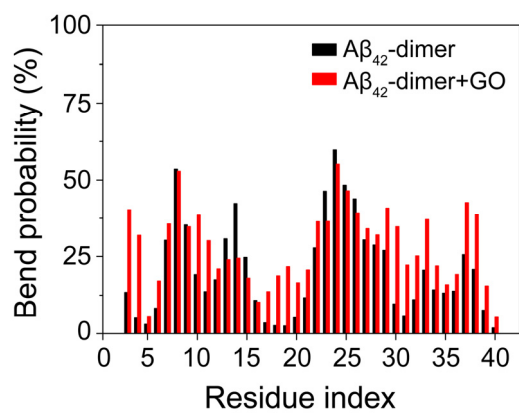


Fig. S12 Residue-based bend probability of the $A\beta_{42}$ dimer in $A\beta_{42}$ -dimer and $A\beta_{42}$ -dimer+GO systems.